MicroBooNE Sterile Neutrino Search through Muon Neutrino Disappearance

Third Year Lab Report

Tavis O'Reilly (10903943)
Department of Physics and Astronomy, University of Manchester
(Experiment performed in collaboration with Eliott Menard)
(Dated: May 2, 2025)

This lab report aims to search for evidence supporting the existence of the sterile neutrino, using data from the Fermilab MicroBooNE experiment. Using machine learning, we categorise the detected particles from their track data, identifying the muon neutrinos (ν_μ). The energy distribution of these ν_μ is then compared to Monte Carlo simulation data which includes the sterile neutrino. The χ^2 of this for different parameters of the sterile neutrino was calculated, excluding a large region of the parameter space at 90% confidence. This coincided well with the inclusion regions at 90% from data gathered in the previous neutrino experiments LSND and MiniBooNE.

1. INTRODUCTION

The MicroBooNE experiment at Fermilab consists of a 170-ton liquid-argon time projection chamber (LArTPC)[1], which allows the detection of neutrinos originating from the Booster Neutrino Beam (BNB). One of the key aims of this expriment is to further investigate the 4.8σ low-energy neutrino excess found in the previous MiniBooNE experiment[2].

One proposed explanation for this excess is a fourth neutrino flavour – the sterile neutrino. Using data from MicroBooNE, we will attempt to exclude regions of the possible parameter space for the properties of this proposed new particle.

2. THEORY

2.1. Neutrino Flavour Oscillation

A neutrino is a type of lepton that only interacts via the weak force. They have three flavours in the Standard Model, labelled ν_e, ν_μ, and ν_τ. Due to the fact that the neutrino flavour and mass eigenstates for the are not the same, a neutrino produced in one flavour state may be detected as a different flavour. The flavour and mass eigenstates are related by the PMNS matrix[3], which for a simple two-flavour model is

$$\begin{pmatrix}\nu_\alpha\\ \nu_\beta\end{pmatrix} = \begin{pmatrix}\cos\theta & \sin\theta\\ -\sin\theta & \cos\theta\end{pmatrix}\begin{pmatrix}\nu_1\\ \nu_2\end{pmatrix}, \tag{1}$$

where θ is the mixing angle between the mass and flavour eigenstates. The flavour components are ν_α and ν_β, and the mass components are ν_1 and ν_2. The probability of a flavour disappearance (a change of flavour away from the original) in this model is given by

$$P(\alpha\to\beta) = \sin^2(2\theta)\sin^2\left(1.27\frac{\Delta m^2_{12}L}{E}\right), \tag{2}$$

where Δm_{12} is the difference in the two neutrino masses in eV, L is the distance travelled in km, and E is the energy of neutrino in GeV.

2.2. Sterile Neutrino

This analysis is investigating the existence of the sterile neutrino, so a four-flavour model is required. The full treatment of this would be complex, so the short-baseline approximation will be used – assuming that the oscillation distance is short, and the sterile neutrino has a much greater mass than the other three neutrinos. This allows most terms of the probability to be dropped.

From this, a formula similar to Equation 2 for the muon neutrino survival probability is obtained.

$$P(\nu_\mu\to\nu_\mu) \approx 1 - \sin^2(2\theta_{\mu\mu})\sin^2\left(1.27\frac{\Delta m^2_{14}L}{E}\right), \tag{3}$$

where $\theta_{\mu\mu}$ is an effective mixing angle for muon neutrino survival, Δm_{14} is the mass difference between the electron and sterile neutrino in eV, and the other symbols have the same meaning as in Equation 2. The electron-sterile neutrino mass difference has been used due to the previously stated assumption that the sterile neutrino has a much greater mass than the other neutrinos. Hence, $\Delta m_{14} \approx \Delta m_{24} \approx \Delta m_{34}$.

Other experiments typically investigate electron neutrino appearance, so $\theta_{\mu e}$ – the effective mixing angle for electron neutrino appearance, is required for better comparison. This can be obtained from $\theta_{\mu\mu}$ through

$$\sin^2(2\theta_{\mu e}) = (1 - |\cos(2\theta_{\mu\mu})|)(1 - |\cos(2\theta_{14})|), \tag{4}$$

where θ_{14} is the electron-sterile neutrino mixing angle. From MicroBooNE data, the best-fit value for this parameter was determined as $\sin^2(2\theta_{14}) = 0.240$[4].

3. EXPERIMENT SETUP

The neutrinos in the BNB are predominantly muon neutrinos. These are sent towards the LArTPC of MicroBooNE, where some will with the argon via the weak interaction, for example a charged current interaction as shown in Figure 1.

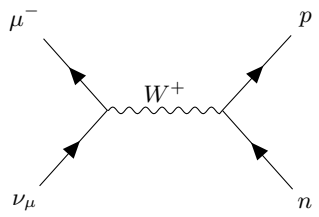

FIG. 1. A Feynmann diagram for a charged current muon neutrino interaction. A muon neutrino exchanges a W^+ boson with a neutron, emitting a muon and a proton.

In this case, the outgoing muon will ionise electrons from nearby atoms, which drift towards the sense wires due to an applied electric field. This produces a current in the sense wires, allowing 3D reconstruction of the muon particle track.

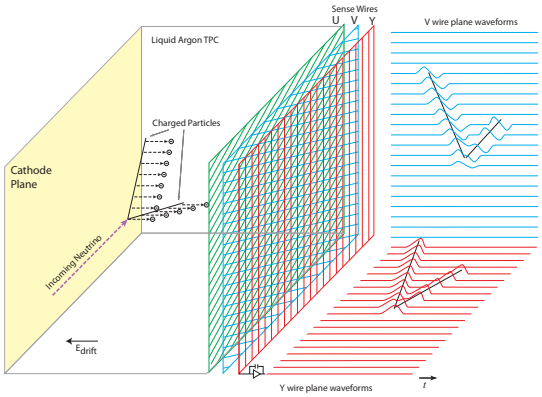

FIG. 2. A diagram showing the setup of the LArTPC and the sense wires used to detect particle tracks. Credit: MicroBooNE collaboration[5].

From this raw track data, a number of direct measurements are made such as: track length, start position, and end position. The initial interaction vertex is also reconstructed as this may not always be at the start of a track[6]. From track data, the neutrino's energy can also be reconstructed. For muon tracks, as shown in Figure 3, they are long and straight, making the muon momentum easy to reconstruct as well.

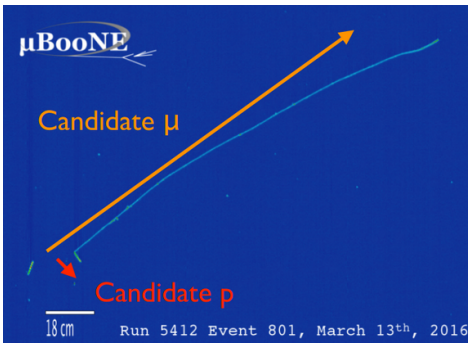

FIG. 3. An example muon track from real data at MicroBooNE. Credit: Fermilab.

Machine learning can be applied to these data points to categorise tracks, enabling the distinction between e.g. cosmic muon tracks, or electron showers (indicating a ν_e). We are interested in detecting ν_μ originating from the beam only, so the machine learning used will focus on identifying this, classifying everything else as background.

4. RESULTS

The preprocessed data from the MicroBooNE experiment includes many of the calculated values discussed previously, along with two machine learning confidence scores between 0 and 1. One for identifying a muon track, and one for identifying an electron shower.

There is also Monte Carlo simulation data, combined with external data (the data gathered when the beam is off). The Monte Carlo data has no flavour oscillation applied, so that this can be varied for different properties of the sterile neutrino.

The first step in the analysis of this data is to make some basic cuts to remove non-physical data (for example where energy couldn't be reconstructed). Also to cut data recorded in the outer-fiducial volume (10 cm around the edge), where edge effects are the most prominent. Beyond this, other cuts can be made to remove regions of the parameter space with a large percentage of background data, as checked in the Monte Carlo simulation data.

More sophisticated analysis involved training a neural network on the Monte Carlo data to identify a ν_μ CC track. With all of the data cuts and the classification of the neural network, the data can be split into signal and background as shown in Figure 4.

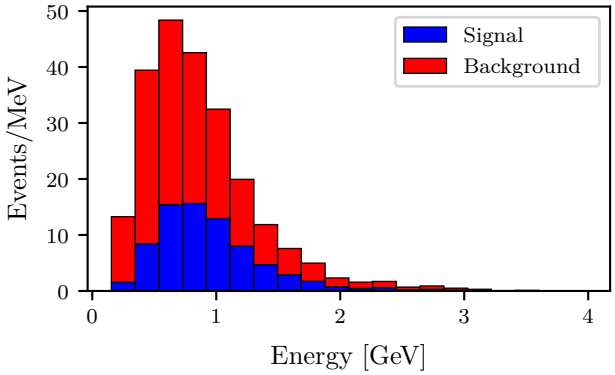

FIG. 4. A histogram plot of how the energy of the detected particles is distributed, showing the categorisation between signal (ν_μ CC interactions) in blue and the background data in red.

With the signal data identified, the Monte Carlo data can be modified to include the survival probability from Equation 3. Calculating the χ^2 between the Monte Carlo and real data, across the parameter space of possible $\theta_{\mu e}$ and Δm^2_{14}, we can exclude regions of the parameter space. A 15% systematic error on the energy is used, along with the Poisson statistical error. The region we excluded is shown in Figure 5.

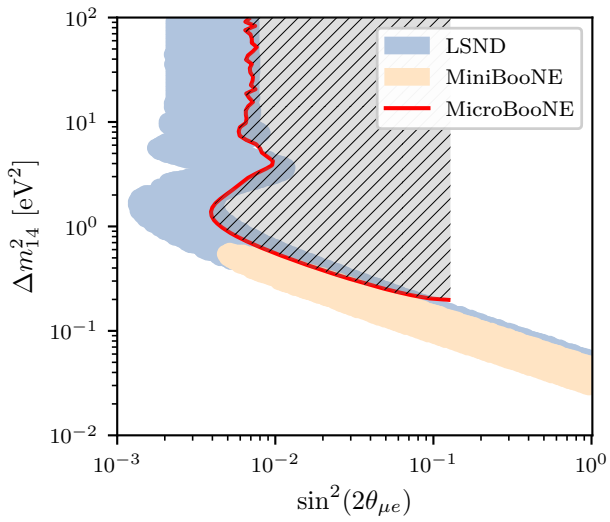

FIG. 5. A plot of the parameter space for the hypothetical sterile neutrino. The possible regions (at 90% confidence) by LSND and MiniBooNE are shown, along with the calculated excluded region at 90% confidence for MicroBooNE data (red line).

5. DISCUSSION

As seen in Figure 5, we have excluded (at 90% confidence) a large region of the parameter space for the sterile neutrino. This region is also in good agreement with the 90% inclusion regions from both LSND and MiniBooNE. Regions towards zero in both parameters could not be excluded due to the nature of the data. The Monte Carlo data was below the real data, and hence any oscillation applied worsened the fit. Despite this, there is a large inclusion region due to the large systematic errors used.

The systematic error was a large limitation of this analysis. The value of 15% is quite high, and also applied uniformly across all energy ranges which is a conservative estimate. If this systematic error could be reduced, more sensitivity, and better exclusion regions could be obtained.

Using muon neutrino disappearance rather than electron neutrino appearance also helps due to the greater number compared to electron neutrinos. This gives greater statistical significance to the results.

6. CONCLUSION

In conclusion, the sterile neutrino still represents promising potential for physics beyond the standard model, attempting to explain the 4.8σ low-energy excess observed in the MiniBooNE experiment. Using muon neutrino disappearance, rather than electron neutrino appearance, we have shown good agreement between our 90% confidence exclusion region, and the 90% inclusion regions of LSND and MiniBooNE.

While this neither proves nor disproves the existence of the sterile neutrino, it provides additional data to help narrow down future searches.

[1] Fermilab, "Microboone experiment." `https://microboone.fnal.gov/`. Accessed: 2025-04-14.
[2] The MiniBooNE collaboration, "Updated miniboone neutrino oscillation results with increased data and new background studies," *Physical Review D*, vol. 103, Mar. 2021.
[3] P. Lipari, "Introduction to neutrino physics," pp. 115–199, 2003.
[4] The MicroBooNE collaboration, "Search for a Sterile Neutrino in a 3+1 Framework using the Wire-Cell Inclusive Charged-Current νe Selection from MicroBooNE," 5 2022.
[5] The MicroBooNE collaboration, "Design and construction of the microboone detector," *Journal of Instrumentation*, vol. 12, p. P02017, Feb. 2017.
[6] The MicroBooNE collaboration, "Neutrino event selection in the microboone liquid argon time projection chamber using wire-cell 3d imaging, clustering, and charge-light matching," *Journal of Instrumentation*, vol. 16, p. P06043, June 2021.